Mathematical Modeling of the Mojave Solar Plants

Antonio J. Gallego [1],*, Manuel Macías [2], Fernando de Castilla [2] and Eduardo F. Camacho [1]

[1] Departamento de Ingeniería de Sistemas y Automática, Universidad de Sevilla, Camino de los Descubrimientos s/n, 41092 Sevilla, Spain; efcamacho@us.es

[2] Atlantica Yield, Albert Einstein s/n, 41092 Sevilla, Spain; manuel.macias@atlanticayield.com (M.M.); fernando.decastilla@atlanticayield.com (F.d.C.)

* Correspondence: gallegolen@hotmail.com or agallego2@us.es; Tel.: +34-954-487-347

Abstract: Competitiveness of solar energy is one of current main research topics. Overall efficiency of solar plants can be improved by using advanced control strategies. To design and tuning properly advanced control strategies, a mathematical model of the plant is needed. The model has to fulfill two important points: (1) It has to reproduce accurately the dynamics of the real system; and (2) since the model is used to test advanced control strategies, its computational burden has to be as low as possible. This trade-off is essential to optimize the tuning process of the controller and minimize the commissioning time. In this paper, the modeling of the large-scale commercial solar trough plants Mojave Beta and Mojave Alpha is presented. These two models were used to test advanced control strategies to operate the plants.

Keywords: solar energy; parabolic trough; modeling; distributed parameter model; black-box models

1. Introduction

Interest in renewable energy sources such as solar energy experienced a great impulse after the Big Oil Crisis in the 1970s. Driven mainly by economic factors, this interest decreased when oil prices fell. Nowadays, there is a renewed interest in renewable energies spurred by the need to reduce the environmental impact produced by the use of fossil energy systems [1,2]. Solar energy is, by far, the most abundant source of renewable energy. In fact, wind and most of the hydraulic energies come from solar energy [3,4].

Many solar energy plants have been commissioned in the last 15 years. As examples, we can mention the three 50 MW Solnova and the two 50 MW Helioenery parabolic trough plants in Spain, and the SOLANA and Mojave Solar parabolic trough plant constructed in Arizona and California, each of 280 MW power production [5,6].

This paper presents the mathematical model of the Mojave Solar Plants Alpha and Beta [6]. The Mojave solar Project (MSP) is a concentrated solar power (CS) facility constructed in the Mojave Desert in California, about 32 km northwest of Barstow. It is owned and operated by Atlantica. It consists of two different parabolic trough plants: Mojave Alpha and Mojave Beta. Both are composed of 282 loops with a peak gross electrical power of 280 MW (140 MW per plant). Large scale parabolic trough plants such as the Mojave facility represent an opportunity and a great challenge from the point of view of modeling and developing advanced control strategies. Section 2 is devoted to a more detailed description of the Mojave solar complex.

Considerable research effort has been developed during the last 30 years concerning the modeling and control of solar power plants. The first works related to the modeling and control were developed for the experimental solar trough plant ACUREX [7–11]. Then, many works concerning the mathematical modeling of solar trough plant have been published, going from first principle models [12,13], where heat transfer equations are used [14], to object oriented modeling using software

such as modelica [15]. There exist also more complex models using software simulation such as Matlab, where every component of the solar plant is modeled in detail to obtain a very realistic response [16,17]. This last approach is very useful to perform economic analysis [18–20] and operators training, but it is not adequate for control and simulation purposes because it is computationally demanding. In general, in the works published providing a comparison between the model response and the real data taken from the plant is not common. In this paper, the model response is compared to the real plant response to evaluate its correctness.

To develop a mathematical model of this kind of plants, two points raised below have to be taken into account:

- To obtain very precise models, a many data are needed to identify all the model coefficients. If there are many coefficients to be identified, the resulting nonlinear optimization problem may be very difficult or even impossible to solve in an adequate time frame. Another important problem is that many coefficients may lead to over-fitting problems. Many data with sufficient dynamics variability would be required . An adequate trade-off between complexity and precision is indispensable, since in real plants the measurable variables are limited and certain variables will not be available.
- The computational time to simulate different environmental conditions and situations should be as fast as possible. If the computational time is high, the optimization of tuning parameters is difficult and the commissioning time of the controller may be delayed. The total computational time for simulating 12 h of operation with the proposed model is about 80 s on a i3 processor with 4 GB of RAM. The model runs on a Matlab® (2014b, Mathworks) simulation environment.

A parabolic trough plant typically consists of a solar field composed of many loops, an energy storage system, a power block and the auxiliary items such as pipes, valves, etc. There are three main elements to be modeled: the solar field, the power block and the pipes connecting them.

The control objective in this kind of plants is to regulate the average of the outlet temperature of the loops around a desired set-point [21]. As mentioned above, to develop as simply a model as possible the following points are followed:

- Solar Field: For both plants, the average temperature of each quadrant forming the whole field is modeled. The final average temperature is the weighted average temperature of all quadrants calculated taking into account the number of loops of every quadrant. This is the variable to be controlled.
- Piping system: The pipes connecting every subsystems are modeled with distributed parameter model equations.
- Steam generator: The steam generator is composed of multiple subsystems. The model developed in this paper does not aim at describing very precisely all the steam generator variables. Only the variables that are useful to the development of the control strategy are modeled.

The main contribution of this paper is twofold:

1. The solar field is composed of 282 loops but modeling 282 loops in parallel would result in a very slow computational model. The amount of data needed for the model would be very high. The approach used in this paper is to consider an equivalent loop within series with a lumped parameter model modeling the additional dynamics of each sector. This approach has not been proposed in the existing literature and has shown a good trade-off between accuracy and computational time. Furthermore, a comparison between the model response and real data taken from the real plant was carried out.
2. As far as the steam generator is concerned, in this paper, a black-box modeling approach is used. In the literature [16,17], the block power is modeled as a simple mathematical equation [22], or as a complete model describing all the power block elements. In this paper, it has been found that

the proposed approach achieves a reasonably good results to model the steam generator variables needed for developing advanced control strategies. Since the resulting equations are very simple, the computational time for the steam generator equations is very low.

More details about modeling are given in the corresponding sections.

The paper is organized as follows. Section 2 presents a description of the Mojave Solar Project. Section 3 presents the model of the solar field. Section 4 describes the model of the pipes connecting the plant subsystems. Section 5 develops the model of the steam generation variables needed to design a control strategy. Finally, the papers draws to a close with concluding remarks.

2. Brief Plant Description

Mojave Solar project is a 280 MW gross utility scale solar thermal electric plant located near Barstow, California. Solar thermal electric technology uses mirrors (parabolic trough collectors) to concentrate solar energy to drive a conventional steam turbine. Figure 1 shows a panoramic view of the Mojave Solar Project [23].

Figure 1. Mojave solar project: Courtesy of Atlantica Yield.

Mojave uses a new parabolic trough technology that is more efficient and cost effective. The project site was configured to minimize environmental impacts and is a model for sustainable development.

Mojave Solar Plants deliver electricity to serve approximately to 75,000 homes and prevent the emission of 423,800 tons of CO_2 to the atmosphere. They contributed to the goal of achieving 33% of overall electricity production from renewable sources by 2020 in California [24].

Mojave Solar project harbors two different and independently operable plants, namely Mojave Alpha and Mojave Beta, which can produce a 140 MW gross power peak each. The solar field of each plant is composed of 282 loops (1128 parabolic trough collectors) covering about 780,000 square meters of reflective area. The collectors concentrate the direct solar radiation onto a tube where a heat transfer fluid is circulating. The electricity generation is provided 100% from the sun. The plants were commissioned at the beginning of December 2014 [25].

3. Mathematical Modeling of the Mojave Alpha and Beta Solar Collector Fields

In this section, the mathematical model of the solar field of both plants Mojave Beta and Mojave Alpha is presented. The mathematical model intends to be used to test control strategies for regulating the temperature of the solar field using the HTF flow as a manipulated variable. It has to be simple but precise.

The control objective in this kind of plants is to regulate the average temperature of the solar field around a desired set-point. The temperature can be obtained as the average outlet temperature of all

loops. However, these two large scale plants have 282 loops each. Modeling 282 loops would be a very difficult task not only for the amount of measurements and parameters needed (some of them may not be available) but also because simulating 282 parallel loops is very demanding from the computational point of view. Testing and optimizing a control strategy would be a very heavy process.

The equations governing the system dynamics are similar to those explained in [26]. There are two ways of modeling this kind of system: the concentrated parameter model and the distributed parameter model [27]. In this paper, the distributed parameter model is used for simulation purposes and the concentrated parameter model is used for control purposes.

The approach used in this paper is to model the average temperature of every sector. A sector is a group of loops. Mojave Beta is composed of seven sectors and Mojave Alpha is composed of four sectors. The final temperature is the weighted mean of the temperature of all sectors.

It is worth pointing out that the advantage of choosing this approach is not only the simplicity and the lesser computational time but that all the measures needed to identify a mathematical model are available. To model a sector, the following variables are needed: the average outlet temperature of the loops, the inlet temperature of the sector, the oil flow, the direct normal irradiance, the number of defocused collectors (to compute the overall optical efficiency) and the average reflectivity.

To model a sector average temperature, two main assumptions are made:

(a) The dynamics of each sector is considered as a one equivalent loop, that is, all the loops forming the quadrant are considered to have the same efficient (the overall efficiency of the quadrant). This assumption is based on the fact that the most efficient loops compensate the less efficient ones. The flow of this equivalent loop is considered to be the mean flow of the sector (flow divided by the number of loops). A distributed parameter model is used to model this equivalent loop.

(b) However, a sector has a great number of loops and the average temperature of the quadrant has an additional dynamics due to different distances from the input of the sector to each loop and the different flows of each loop. After performing an analysis, it was found that this dynamics can be modeled as a lumped parameter model with a determined area, length and a thermal losses coefficient. The flow of this model is equal to the flow of the whole sector.

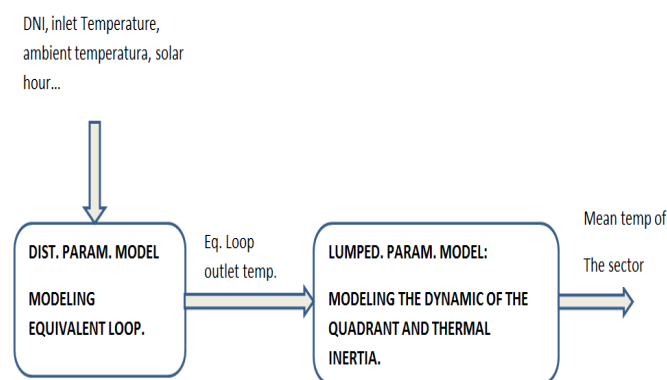This way of modeling the solar field can be observed in Figure 2.

Figure 2. Modeling procedure for a sector.

To understand better how the solar plant works, Figure 3 shows the scheme of how the solar field is connected to the steam generator. HTF is heated up in the solar field and then is delivered to the steam generator trough the pipe connecting both. HTF is used to produce electricity in a turbine by means of a steam generator. HTF transfers heat and, consequently, its temperature decreases. The steam generator returns the cold oil to the solar field to be heated up again and repeat the process.
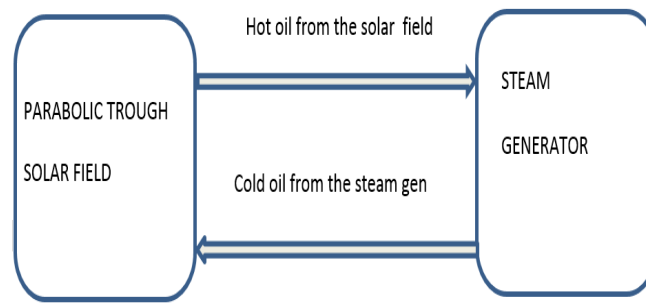
Figure 3. Solar plant scheme.

Subsequently, the distributed and concentrated parameter model equations are described.

3.1. Distributed Parameter Model

In this subsection, the equations governing the distributed parameter model are presented. As mentioned above, the sector dynamics is modeled as an equivalent loop in series with a concentrated parameter model modeling the thermal inertia of the whole sector.

A loop of the Mojave solar plants consists of a set of parabolic trough collectors which concentrate solar radiation onto a line where an absorption tube is placed. The model is described by the following system of partial differential equations (PDE) describing the energy balance [11,26]:

$$\rho_m C_m A_m \frac{\partial T_m}{\partial t} = IK_{opt}cos(\theta)G - H_l G(T_m - T_a) - LH_t(T_m - T_f) \tag{1}$$

$$\rho_f C_f A_f \frac{\partial T_f}{\partial t} + \rho_f C_f q \frac{\partial T_f}{\partial x} = LH_t(T_m - T_f) \tag{2}$$

where m subindex refers to metal and f subindex refers to a fluid. In Table 1, parameters and their units are shown.

Table 1. Parameters description.

Symbol	Description	Units
t	Time	s
x	Space	m
ρ	Density	kgm^{-3}
C	Specific heat capacity	JK^{-1}kg^{-1}
A	Cross sectional area	m^2
$T(x,y)$	Temperature	K,°C
$q(t)$	HTF flow rate	m^{3}s^{-1}
$I(t)$	Direct Solar radiation	Wm^{-2}
$cos(\theta)$	geometric efficiency	Unitless
K_{opt}	Optical efficiency	Unitless
G	Collector aperture	m
$T_a(t)$	Ambient temperature	K,°C
H_l	Global coefficient of thermal loss	Wm^{-2}°C^{-1}
L	Length of pipe line	m
$H_t(t,T,q)$	Coefficient of heat transmission metal-fluid	Wm^{-2}°C^{-1}
S	Total reflective surface	m^2
$C_T(t,T)$	Thermal capacity of the whole sector	J/K
H_{lc}	Lumped parameter model global coefficient of thermal loss	Wm^{-2}°C^{-1}

The PDE system is solved by dividing the metal and fluid in 260 segments of 2 m long. The integration step is chosen of 0.5 s.

The optical efficiency, K_{opt}, takes into account elements such as reflectivity, metal absorptance, interception factor and others.

3.1.1. Computation of the Geometric Efficiency

The geometric efficiency, $cos(\theta)$, is determined by the position of the collectors with respect to the sun vector. It depends on hourly angle, solar hour, declination, Julianne day, local latitude and collector dimensions [1,28].

Commercial solar parabolic trough plants track the sun using N-S orientation [29]. The variable $cos(\theta)$ can be computed as follows [30].

$$cos(\theta) = \sqrt{cos(\theta_z)^2 + cos(\delta)^2 sin(\omega)^2} \tag{3}$$

where δ is the declination and it can be obtained using the well known Spencer formulas by using Equation (4), [11].

$$\delta = 0.006918 - 0.399912 \cdot cos(\omega) + 0.070257 \cdot sin(\omega) - 0.006758 \cdot cos(2 \cdot \omega) + 0.000907 \cdot sin(2 \cdot \omega)$$
$$- 0.002697 \cdot cos(3 \cdot \omega) + 0.00148 \cdot sin(3 \cdot \omega) \tag{4}$$

The variable ω is the hourly angle, the angular displacement of the sun east or west of the local meridian due to rotation of the Earth on its axis at 15 degrees per hour. It can be calculated as follows:

$$\omega = (T_{sun} - 12) \cdot 15 \cdot (\Pi/180) \tag{5}$$

where T_{sun} is the solar hour [31], which can be computed using the local time as follows [32]:

$$T_s = localhour + 4(L_{st} - L_{loc}) + E_t$$

where L_{st} is the standard meridian for the local time zone, L_{loc} is the longitude of the location in degrees west and E_t is the equation of time (in minutes), which can be obtained using Equation (6):

$$E_t = (0.000075 + 0.001868 \cdot cos(B) - 0.032077 \cdot sin(B) - 0.014615 \cdot cos(2 \cdot B)$$
$$- 0.04089 \cdot sin(2 \cdot B)) \cdot 229.18 \tag{6}$$

B computed as $B : (2\pi/365) \cdot (JD - 1)$, where JD is the Julianne day.

The zenith angle is denoted by θ_z, the angle of incidence of beam radiation on a horizontal surface [30]. It can be obtained by using the expression (7):

$$\theta_z = cos(\phi)cos(\delta)cos(\omega) + sin(\phi)sin(\delta) \tag{7}$$

The variable ϕ stands for the latitude.

3.1.2. Heat Transfer Fluid Properties

The plants use as a heat transfer fluid (HTF) Therminol VP1 oil. HTF is a highly stable, long-lasting silicone fluid designed for high temperature liquid phase operation [33].

The density ρ_f, specific heat C_f, and coefficient of heat transmission have been adjusted by using data from the manufacturer datasheet. A polynomial adjustment has been carried out to obtain expressions valid in the entire operating range. The expressions are given by Equations (8) and (9):

$$\rho_f = -9.0242e - 4\ T_f^2 - 0.5787\ T_f + 1061.5\ (\text{kg/m}^3) \tag{8}$$

$$C_f = 0.0010558T_f^2 + 2.38501T_f + 1552.049 \ (J/(kg\,^\circ C)) \tag{9}$$

Obtaining the heat transmission coefficient is a bit trickier. It is composed of two parts, one depending on the fluid temperature and the other on the flow-rate [34]. Obtaining the expression of this coefficient involves using complex convection heat transmission formulas [35].

The expressions are as follows:

$$Hv(T) = 2 \cdot (7.182817e - 7T_f^4 - 1.356114e - 3T_f^3 + 0.267921T_f^2 + 479.1142T_f + 5.011334e3 \tag{10}$$

$$H_t = Hv(T)q^{0.8} \ (W/(m^2\,^\circ C)) \tag{11}$$

3.1.3. Thermal Losses Coefficient

The global thermal losses coefficient has been estimated by using experimental data from the real solar field. An important point to be stressed is that this coefficient represents the average coefficient of a particular sector. To obtain an expression for this coefficient, the following expression has been chosen [36,37] (Equation (12)):

$$H_l = a_1(T_m - T_a)^3 + a_2(T_m - T_a)^2 + a_3(T_m - T_a) +$$
$$+ a_4 \frac{1}{(T_m - T_a)} \tag{12}$$

where T_m is the metal temperature of a particular segment, T_{amb} is the ambient temperature and the coefficients $a_1...a_4$ have to be obtained using real data.

3.2. Concentrated Parameter Model

A concentrated parameter model provides a lumped description of the whole sector [38,39]. In this paper, this equation is used to model the dynamics of the whole sector, as explained above.

The variation in the internal energy of the fluid can be described by the equation:

$$C_T \frac{dT_{out}}{dt} = K_{opt}cos\phi SI - q\,C_f\rho_f(T_{out} - T_{in}) - \tag{13}$$
$$- H_{lc}S(\bar{T} - T_a)$$

where q is the HTF flow of the whole sector and T and T_{in} are the outlet and inlet oil temperatures, respectively, of the model. The outlet temperature of the lumped parameter model T is the final average temperature of the sector and T_{in} is the outlet temperature of the distributed parameter model.

The variable $\bar{T}$ is the average value between inlet and outlet temperatures and T_a is the ambient temperature. C_T is the thermal capacity of the sector, K_{opt} is the optical efficiency (which incorporates the effects of mirror reflectivity, tube absorptance, and interception factor), I is the direct solar irradiance and S is the total reflective surface, which depends on the number of loops that form the sector.

3.3. Comparison between Model and Real Responses

In this section, a comparison between model and real responses is presented. For the sake of brevity, not all sectors' temperature evolutions are presented. Firstly, results belonging to the Mojave Beta plant are shown and then the same is done for Mojave Alpha. All results in this and the next sections are scaled between 0 and 1. The real data cannot be provided due to confidentiality and intellectual property issues.

Mojave Beta solar trough plant is composed of six sectors: east (42 loops), north-east (46 loops), north-west (38 loops), south-east (40 loops), south-west (38 loops) and west (78 loops). Figure 4 shows the comparison between the model output and the real average temperature of the Mojave Beta East

sector. It is a transient day where passing clouds are affecting the sector. As can be seen, the dynamics of the model is quite similar to that of the real sector evolution.
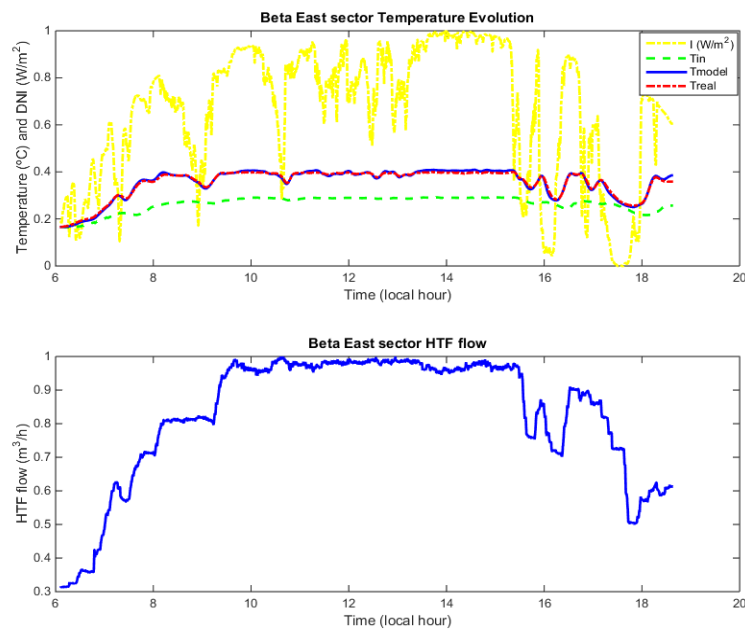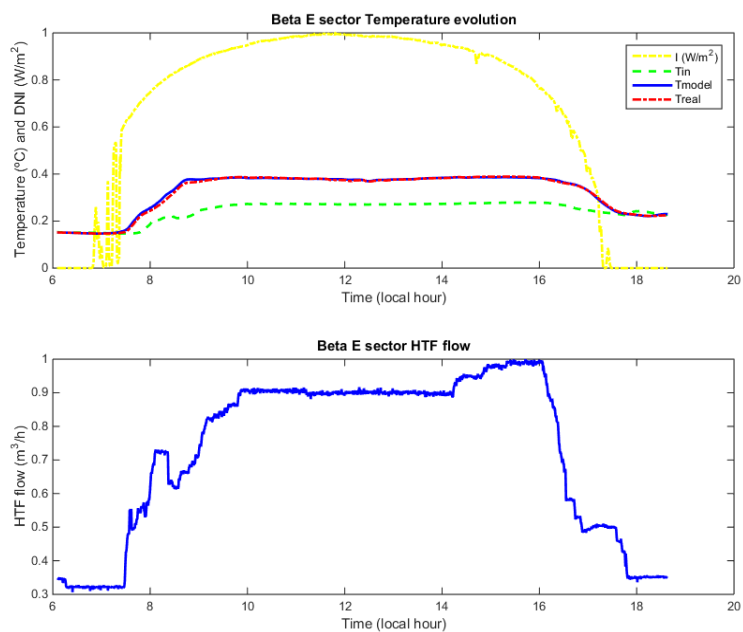

Figure 4. Beta East sector, model vs. real evolution: (**top**) model (blue solid) and real (red dash-dotted); and (**bottom**) HTF flow.

Similar comments can be done about the comparisons between the model and real temperatures shown in Figure 5. In the figure, the evolution of the Beta North-East and Beta South-East temperatures are compared to the evolution of the corresponding models. The models replicate properly the evolution of the measured temperature.

Figure 5. Beta North-East sector, model vs. real evolution: (**top**) model (blue solid) and real (red dash-dotted); and (**bottom**) HTF flow.

Finally, Figure 6 shows the average temperature of the whole Beta solar field and the weighted average of all the sectors model. As can be seen, the model evolution is very close to the real temperature.
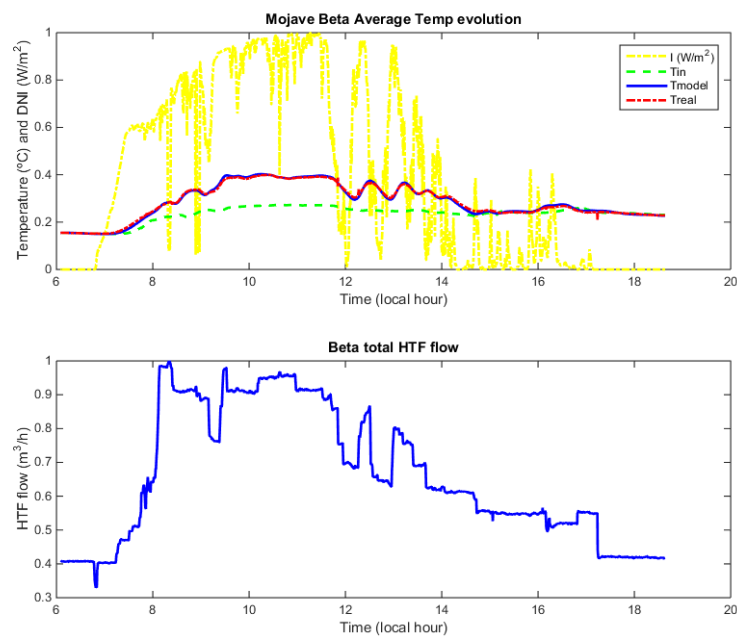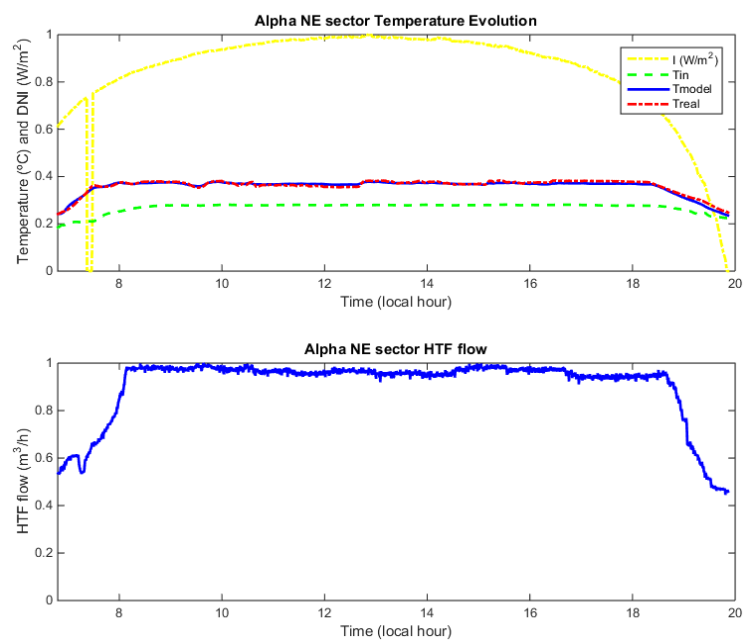

Figure 6. Beta average temperature, model vs. real evolution: (**top**) model (blue solid) and real (red dash-dotted); and (**bottom**) HTF flow.

Mojave Alpha solar trough plant consists of four sectors: north-west (68 loops), north-east (20 loops), east (102 loops) and west (92 loops). Figure 7 presents the evolution of the Alpha North-East sector in a clear day of summer. As can be seen, the evolution of the model is very similar to that of the real sector.

Figure 7. Alpha North-East sector, model vs. real evolution: (**top**) model (blue solid) and real (red dash-dotted); and (**bottom**) HTF flow.

Figure 8 shows the comparison between the model of the Alpha West sector evolution and the real sector temperature in a clear day of winter. The model evolution follows properly the real one.
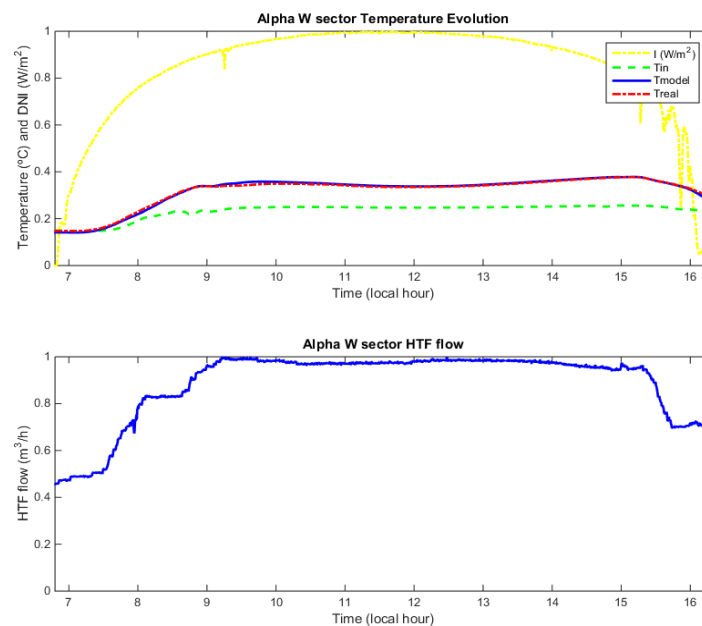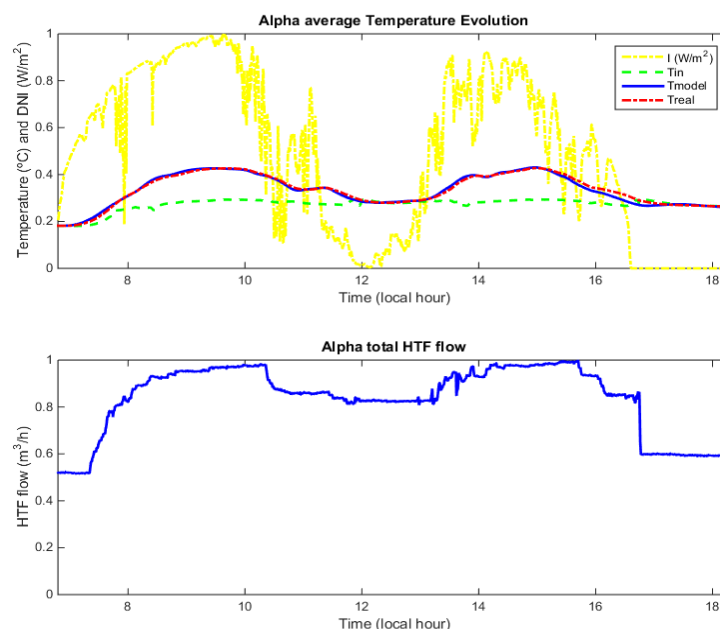

Figure 8. Alpha West sector, model vs. real evolution: (**top**) model (blue solid) and real (red dash-dotted); and (**bottom**) HTF flow.

In Figure 9, the evolution of the average temperature of the Alpha solar trough plant on a cloudy day is presented. As can be seen, the model evolution is quite similar to the measured temperature.

Figure 9. Alpha average temperature, model vs. real evolution: (**top**) model (blue solid) and real (red dash-dotted); and (**bottom**) HTF flow.

This section shows that the mathematical model of the Mojave Alpha and Beta solar field works properly on both clear days and days with passing clouds.

To make a more precise analysis of the model behavior, a table containing the maximum error in percentage between the model response and the real data taken from the field has been obtained. The analysis was done for the two plants Alpha and Beta.

As can be seen in Table 2, the maximum error obtained is about a 6.1%, which constitutes an acceptable result considering that there are many error sources such as shade factors affecting the field in the start-up and the sunset situations, or the radiation provided by pyrheliometers, which is a punctual measurement and may not be representative of the real solar radiation affecting the whole sector. In fact, on transient days, there can be loops affected by a passing cloud while others are not and vice versa. In this model, the solar radiation considered is that measured by the pyrheliometer. Despite this, and since the objective of the models presented here is to be used for developing control strategies and not to be a very accurate model, the result can be considered satisfactory.

Table 2. Maximum error between the model output and the real data.

Mojave Beta	East Sector	NE Sector	Average Temp.
Maximum error (%)	5.41	6.01	4.96
Mojave Alpha	NE Sector	W Sector	Average temp.
Maximum error (%)	5.1	6.1	4.95

4. Modeling of the Piping System

In this section, the mathematical modeling of the pipes connecting the plant subsystems is presented. There are three types of pipes in the solar plants:

(a)　The pipe which connects the solar field to the steam generator.
(b)　The pipe which connects the steam generator to the main oil pumps.
(c)　Pipes which connect the oil pump to the input of every sector.

For modeling purposes, the pipe connecting the steam generator to the main oil pumps is not modeled, because it is very short compared to the other pipes. The pumps temperature is considered to be the returned HTF temperature of the steam generator.

The equations of the pipe modeling are the same as those presented for the distributed parameter model, but considering the irradiance equal to 0. The system of partial differential equations are given by Equations (15):

$$\rho_m C_m A_m \frac{\partial T_m}{\partial t} = -H_l G(T_m - T_a) - L H_t (T_m - T_f) \tag{14}$$

$$\rho_f C_f A_f \frac{\partial T_f}{\partial t} + \rho_f C_f q \frac{\partial T_f}{\partial x} = L H_t (T_m - T_f) \tag{15}$$

The parameter to be identified are the cross sectional Area A_f, the total length of the pipe and the coefficient of the thermal losses H_l.

Figures 10 and 11 show a comparison between the model output of the pipe connecting the solar field and the steam generator, and the HTF temperature measured at the input of the steam generator. As can be seen, the model evolution is quite close to the real measurement.
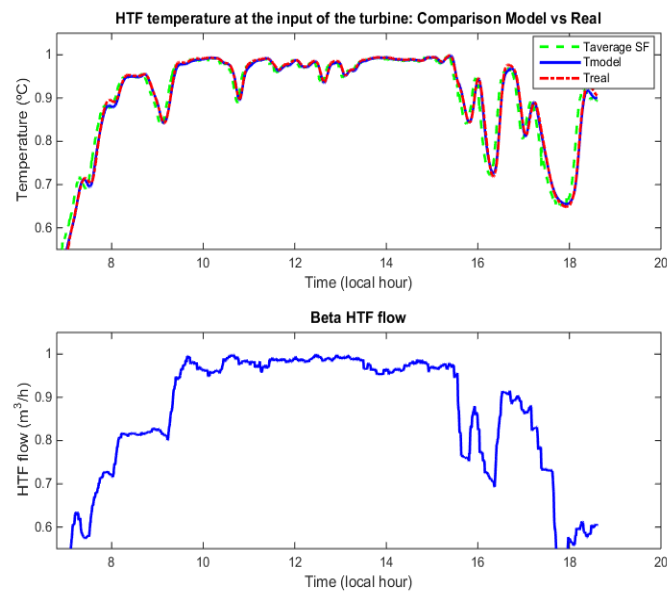
Figure 10. Mojave Beta, HTF temperature at the input of the Steam generator: (**top**) model (solid blue) and real (red dash-dotted); and (**bottom**) HTF flow.

As far as the pipes connecting the oil pumps and the input of every sector, two figures showing a comparison between the model and the real measurement for two sectors are provided. The rest of the models are quite similar.
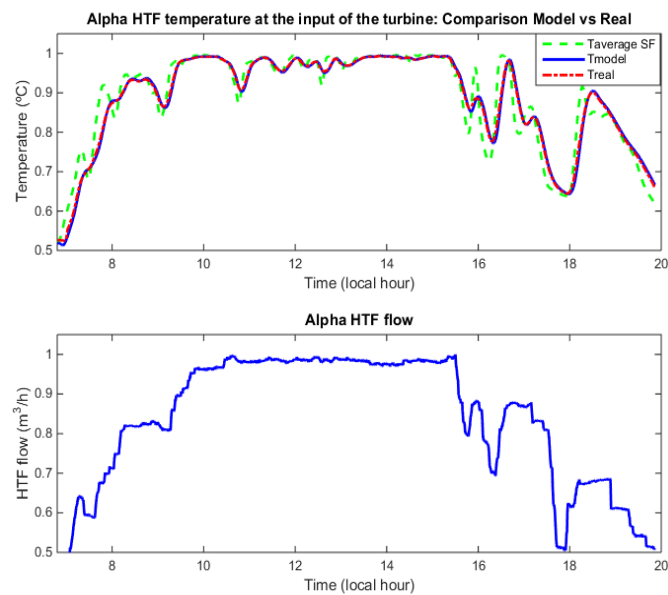

Figure 11. Mojave Alpha, HTF temperature at the input of the Steam generator: (**top**) model (solid blue) and real (red dash-dotted); and (**bottom**) HTF flow.

Figure 12 shows the evolution of the pipe model which connect the oil pumps and the inlet of the sector West. As can be seen, the model captures well the real pipe dynamics. Figure 13 shows a comparison between the model of the pipe connecting the pumps and the North-West sector. As can be observed, the model replicates properly the real pipe behavior.
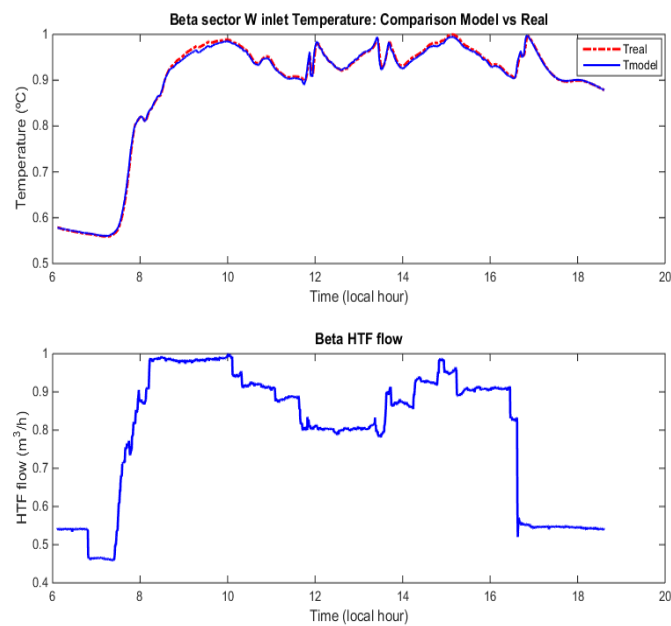
Figure 12. Mojave Beta, inlet temperature of the west sector: (**top**) model (solid blue) and real (red dash-dotted); and (**bottom**) HTF flow.
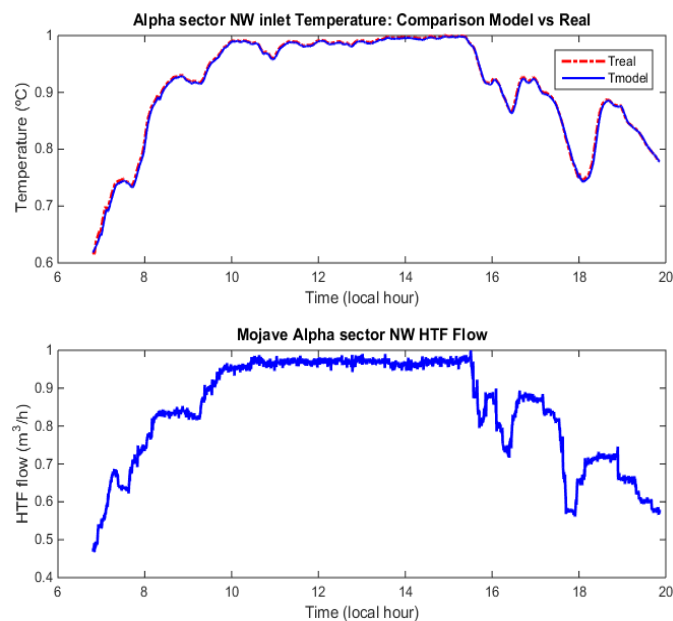

Figure 13. Mojave Alpha, inlet temperature of the North-West sector: (**top**) model (solid blue) and real (red dash-dotted); and (**bottom**) HTF flow.

To evaluate the model accuracy compared to the real data, Table 3 contains the maximum error in percentage for the tests presented. As can be seen, the maximum error produced by the model output is about 3.8%, which is an acceptable result considering the model goal.

Table 3. Maximum error between the model output and the real data.

Mojave Beta	Solar Field to Turbine Pipe	Turbine-Input of the Solar Field
Maximum error (%)	2.86	2.1
Mojave Alpha	Solar Field to Turbine pipe	Turbine-Input of the solar field
Maximum error (%)	3.86	1.5

5. Modeling of the Steam Generator Variables

In this section, the steam variables useful for simulation and tuning the controller parameters are modeled. The models of this part usually are very complicated and they need a great deal of data for parameters to be identified since the power block, the set steam generator + turbine, is composed of many elements [40]. The modeling can be addressed by using object oriented languages such as modelica if a very detailed model is needed. In [41], a complex model developed in modelica of a CSP power plant is presented. In that work, all the components of the power block are modeled. In [42], a complex and detailed model developed in TRNSYS of the steam generator is presented to study the start-up stage. In [40], a complex model of a steam turbine is developed. The model parameters were identified using a genetic algorithm.

Since the purpose of this work is obtaining models to be used in a simulator to test and tune advanced control strategies, simple models are adequate. The objective of the model is not to develop a very precise model of every part composing the power block but to obtain a model only for the variables needed to be used in future control strategies.

To address this issue, a black-box approach is used [43]. In this kind of models, the output is a function of the inputs, but the model structure is unknown a priori [44]. The model structure is chosen based on experience. To avoid the over-parameterization, only data for five days of operation are used to obtain the model parameter. The model output is then compared with all the data available to find if it works well in all conditions. The steam variables needed to simulate advanced control strategies are the following: steam temperature, high pressure, gross power, HTF return temperature, the steam temperature gradient and the superheating temperature. The models of these variables are explained below.

One further comment should be made: although the models structure are not known, to figure out what variables are more suitable to be included in a particular model structure, a correlation analysis was carried out.

5.1. Steam Temperature Mathematical Model

To obtain a model for the steam temperature, a first-order dynamic model is chosen. The evolution of this model depends on the HTF temperature of the steam generator, the oil flow and the ambient temperature as follows (Equation (16)):

$$T_{steam}(k) = a_1 \, T_{steam}(k-1) + a_2 T_{HTF} + a_3 q_{HTF} T_{HTF} + a_4 (T_{HTF} - T_a) + a_5 (T_{HTF} - T_a)^2 + a_6 \quad (16)$$

$T_{steam}(k)$ is the steam temperature at instant k. T_{HTF} is the HTF temperature at the input of the steam generator, q_{HTF} is the oil flow reaching the steam generator and T_a is the ambient temperature.

Constants a_1–a_6 have to be obtained. A comparison between the model and real data is shown in Figure 14 for Mojave Beta (Figure 14, top) and Mojave Alpha (Figure 14, bottom). As can be seen, the model evolution is quite close the real measurement.
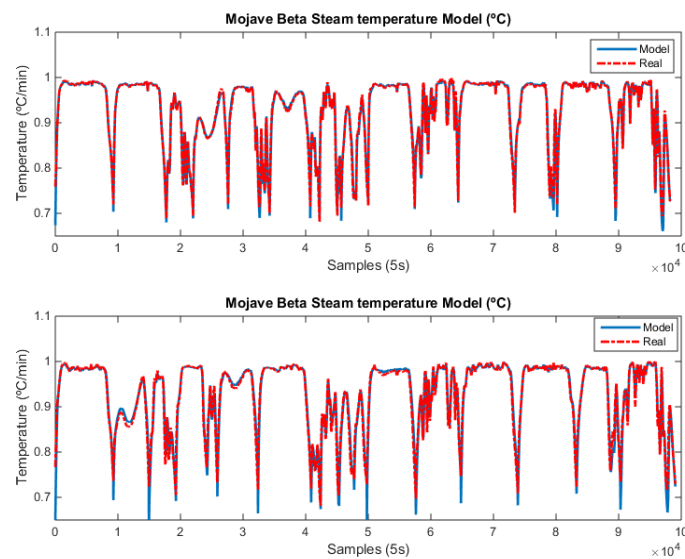
Figure 14. Mojave Beta and Alpha: Steam temperature model: (**top**) Mojave Beta model showing real evolution (red dash-dotted) and model output (blue solid); and (**bottom**) Mojave Alpha model showing real evolution (red dash-dotted) and model output (blue solid).

5.2. High Steam Pressure Model

One of the most important variables in the steam generator is the high steam pressure. This variable has to be supervised and controlled to avoid dangerous situations, including shutdowns of the plant. The structure of the model is chosen based on the fact that the steam pressure depends on the temperature and the flow. The model structure is as follows (Equation (17)):

$$Pressure_{HP}(k) = a_1 T_{steam} + a_2 T_{steam}^2 + a_3 q_{HTF} T_{HTF} + a_4 \qquad (17)$$

A comparison between real data and the model is shown below. Figure 15 shows the comparison between the model and the measured HP Pressure for Mojave Beta (Figure 15, top) and Mojave Alpha (Figure 15, bottom). The model replicates properly the real pressure evolution in both cases.
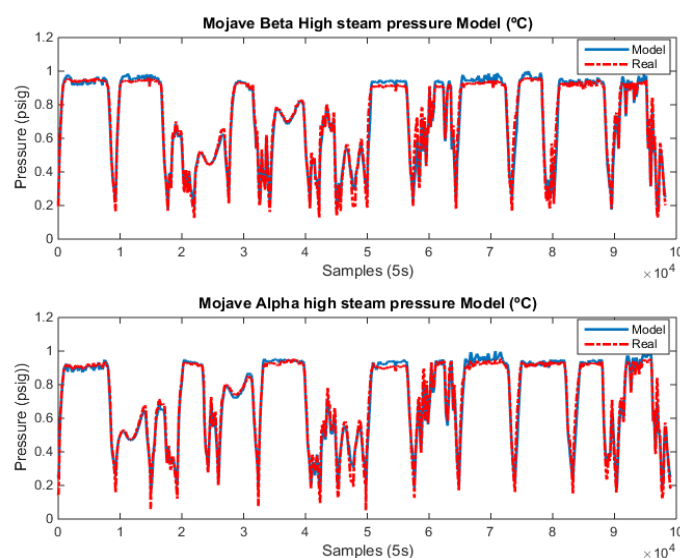

Figure 15. Mojave Beta and Alpha: HP Pressure Model: (**top**) Mojave Beta model, showing real evolution (red dash-dotted) and model output (blue solid); and (**bottom**) Mojave Alpha model, showing real evolution (red dash-dotted) and model output (blue solid).

5.3. Gross Power Mathematical Model

In this subsection, the model of the gross power is presented. The gross power evolution depends on the HP pressure, the steam temperature and the ambient temperature. The model structure chosen is shown in Equation (18):

$$Power_{Gross}(k) = a_1 Pressure_{HP} + a_2(T_{steam} - T_a) \tag{18}$$

Figure 16 shows a comparison between real data and the model output is shown below. Figure 16 (top) shows the model for Mojave Beta and Figure 16 (bottom) shows the comparison for Mojave Alpha. As can be seen, both models fit quite well the real data.
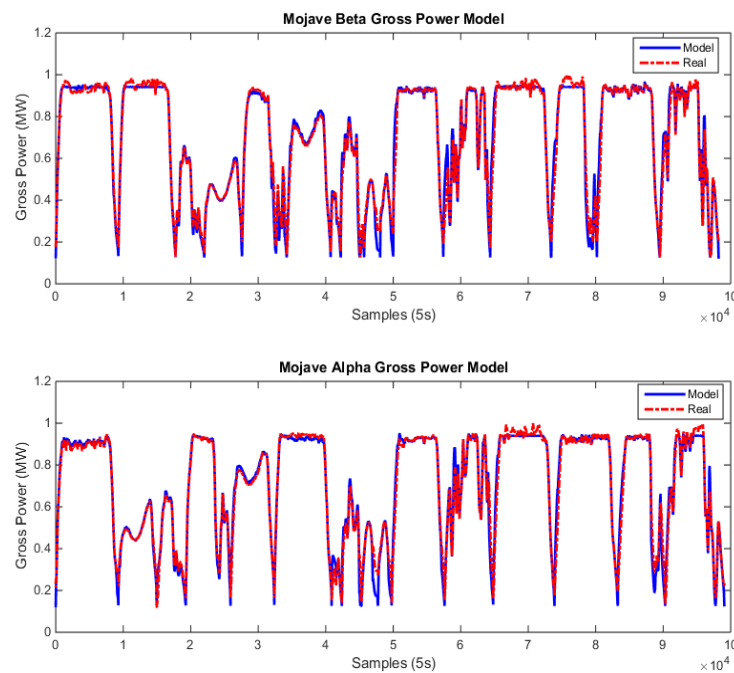

Figure 16. Mojave Beta and Alpha: Gross Power Model: (**top**) Mojave Beta model, showing real evolution (red dash-dotted) and model output (blue solid); and (**bottom**) Mojave Alpha model, showing real evolution (red dash-dotted) and model output (blue solid).

5.4. Oil Pumps Temperature

In this subsection, the oil pumps temperature is modeled. This temperature is essential because it is the HTF temperature returned by the steam generator so that it allows the connection of the steam generator to the solar field.

It is worth noting that this temperature does not correspond exactly with the returned HTF temperature, but, since the oil pumps are near the steam generator, the two temperatures are almost the same. The chosen structure for the model is given by Equation (19):

$$T_{pumps}(k) = a_1 T_{pumps}(k-1) + a_2(T_{steam}) a_3 Power_{Gross} + a_4 Pressure_{HP} + a_5 \tag{19}$$

A comparison between real data and the model is shown in Figure 17. As can be seen, both models are quite close to the real data obtained from the plants. The models can be considered satisfactory.
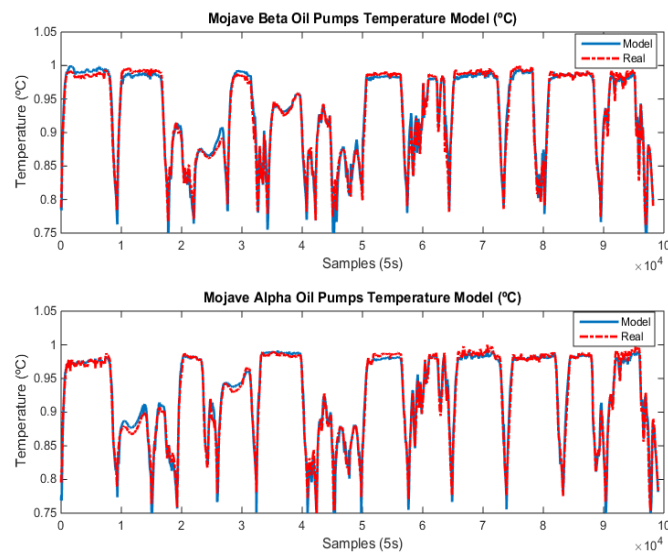
Figure 17. Mojave Beta: Oil Pumps Temperature: (**top**) Mojave Beta model, showing real evolution (red dash-dotted) and model output (blue solid); and (**bottom**) Mojave Alpha model, showing real evolution (red dash-dotted) and model output (blue solid).

5.5. Steam Temperature Gradient

The steam gradient is one of the two variables that a control strategy has to check. A very high value of the steam temperature gradient causes dangerous situations. After a thorough analysis, it has been found that the steam temperature gradient can be modeled using the structure provided by Equation (20)

$$Grad_{steam} = a_1 + a_2 \frac{dPower_{gross}}{dt} + a_3 \frac{dT_{steam}}{dt} \tag{20}$$

A comparison between real data and the model for both plants is shown in Figure 18. As can be seen, the model behaves well and its evolution is quite similar to the real one.
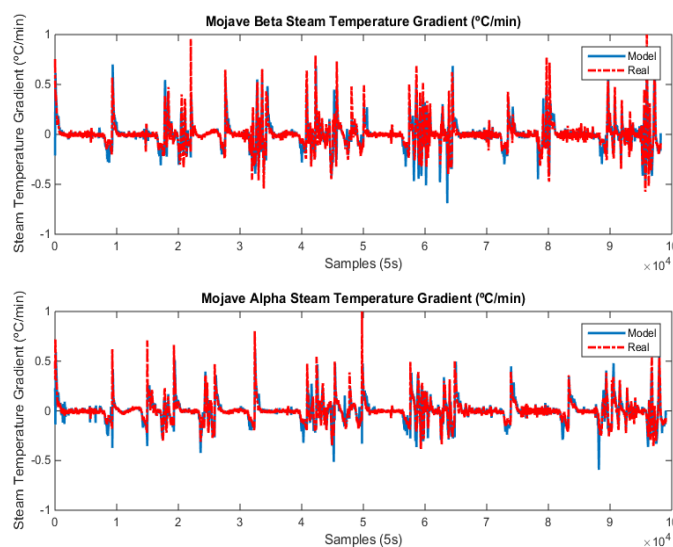

Figure 18. Mojave Beta and Alpha: Steam Temperature Gradient: (**top**) Mojave Beta model, showing real evolution (red dash-dotted) and model output (blue solid); and (**bottom**) Mojave Alpha model, showing real evolution (red dash-dotted) and model output (blue solid).

5.6. Evaluation of the Models

In this subsection, a similar analysis to those developed in the previous sections has been carried out. In this case, greater numerical errors are obtained due to two facts: (i) the simplicity of the proposed models; and (ii) the difficulty to capture the dynamics of the multiple components of the steam generator. Since the aim of the steam generator variables is to obtain a similar behavior to that observed in the real system and not to obtain a very precise model, the important factor is the mean absolute error and not the maximum error. The maximum error may take a high value in a particular moment but then the error between the model and real data decreases substantially. The most difficult variable to be modeled is the steam temperature gradient, which shows the greater error.

Table 4 shows the obtained mean absolute errors (in percent) between the models and real data. As can be seen, despite the simplicity of the proposed models, the result is acceptable.

Table 4. Mean absolute error between the model output and the real data (in percentage).

Plant	Steam Temp.	G. Power	HP Pressure	Oil Pumps Temp.	Steam Temp.Grad	Superheating
Mojave Beta	0.71	5.31	5.03	0.78	15.6	0.23
Mojave Alpha	1.03	5.31	5.12	1.03	17.1	0.22

6. Conclusions

To develop advanced control strategies for solar energy plants, a mathematical model is needed. The model has to fulfill two important issues: (1) it has to reproduce accurately the dynamics of the real system; and (2) since the model is used to test advanced control strategies, its computational burden has to be as low as possible. This trade-off is essential to optimize the tuning process of the controller and minimize the commissioning time.

In this paper, the modeling of the Mojave Solar Trough Plants Alpha and Beta is presented. Three subsystems were modeled: the solar field, the steam variables and the piping system. Abundant results comparing the evolution of the model to the evolution of the real system are shown. They cover multiple operation situations from the clear days to days with passing clouds and strong transients. All subsystems models capture well the dynamics of the real system despite the simplicity aimed. The total computational time for simulating 12 h of operation is about 80 s in a i3 processor with 4 GB of RAM.

Furthermore, a numerical analysis of the errors obtained between the models output and the real data is included showing that the models accuracy is sufficient to use these models for testing and designing advanced control strategies. The final outcome can be considered satisfactory.

Conflicts of Interest: The authors declare that no conflict of interests exists.

Abbreviations

The following abbreviations are used in this manuscript:

HTF	Heat Transfer Fluid
MSP	Mojave Solar Project
PDE	Partial Differential Equations

References

1. Goswami, D.Y.; Kreith, F.; Kreider, J.F. *Principles of Solar Engineering*, 2nd ed.; Taylor&Francis: London, UK, 2000.
2. Camacho, E.F.; Berenguel, M. Control of Solar Energy Systems. In Proceedings of the 8th IFAC Symposium on Advanced Control of Chemical Processes, Singapore, 10–13 July 2012; pp. 848–855.
3. Camacho, E.F.; Gallego, A.J. Optimal Operation in Solar Trough Plants: A case study. *Sol. Energy* **2013**, *95*, 106–117. [CrossRef]
4. Islam, M.T.; Huda, N.; Abdullah, A.B.; Saidur, R. A comprehensive review of state-of-the-art concentrating solar power (CSP) technologies: Current status and research trends. *Renew. Sustain. Energy Rev.* **2018**, *91*, 987–1018. [CrossRef]
5. Solana Generating Station. 2018. Available online: https://solarpaces.nrel.gov/solana-generating-station (accessed on 1 September 2019).
6. Mojave Solar Project. 2018. Available online: https://solarpaces.nrel.gov/mojave-solar-project (accessed on 1 September 2019).
7. Camacho, E.F.; Rubio, F.R.; Berenguel, M. *Advanced Control of Solar Plants*; Springer-Verlag: London, UK, 1997.
8. Lemos, J.M.; Neves-Silva, R.; Igreja, J.M. *Adaptive Control of Solar Energy Collector Systems*; Springer-Verlag: Basel, Switzerland, 2014.
9. Rubio, F.R.; Camacho, E.F.; Berenguel, M. Control de campos de colectores solares. *RIAI* **2006**, *3*, 26–45.
10. Álvarez, J.D.; Costa-Castelló, R.; Berenguel, M.; Yebra, L.J. A repetitive control scheme for distributed solar collector field. *Int. J. Control* **2010**, *83*, 970–982. [CrossRef]
11. Camacho, E.F.; Berenguel, M.; Rubio, F.; Martínez, D. *Control of Solar Energy Systems*; Springer-Verlag: London, UK, 2012.
12. Bishoyia, D.; Sudhakara, K. Modeling and performance simulation of 100 MW PTC based solar thermal power plant in Udaipur India. *Case Stud. Therm. Eng.* **2017**, *10*, 216–226. [CrossRef]
13. Manenti, F.; Ravaghi-Ardebili, Z. Dynamic simulation of concentrating solar power plant and two-tanks direct thermal energy storage. *Energy* **2013**, *55*, 89–97. [CrossRef]
14. de Oliveira Siqueira, A.M.; Neves-Gomesa, P.E.; Torrezania, L.; Lucasa, E.O.; da Cruz-Pereira, G.M. Heat transfer analysis and modeling of a parabolic trough solar collector: An analysis. *Energy Procedia* **2014**, *57*, 401–410.
15. Yebra, L.J.; Berenguel, M.; Bonilla, J.; Roca, L.; Dormido, S.; Zarza, E. Object-oriented modelling and simulation of ACUREX solar thermal power plant. *Math. Comput. Model. Dyn. Syst.* **2010**, *16*, 211–224. [CrossRef]
16. Barcia, L.A.; Menéndez, R.P.; Esteban, J.M.; Prieto, M.A.; Martín, J.A.; de Cos, F.J.; Reviriego, A.N. Dynamic Modeling of the Solar Field in Parabolic Trough Solar Power Plants. *Energies* **2015**, *8*, 13361–13377. [CrossRef]
17. Vergura, S.; Fronzo, V.D. Matlab based Model of 40-MW Concentrating Solar Power Plant. In Proceedings of the International Conference on Renewable Energies and Power Quality (ICREPQ 12), Santiago de Compostela, Spain, 28–30 March 2012; pp. 1259–1263.
18. Rohani, S.; Fluri, T.; Dinter, F.; Nitz, P. Modelling and simulation of parabolic trough plants based on real operating data. *Sol. Energy* **2017**, *158*, 845–860. [CrossRef]
19. Shahnazari, M.R.; Lari, H.R. Modeling of a solar power plant in Iran. *Energy Strategy Rev.* **2017**, *18*, 24–37. [CrossRef]
20. Dua, E.; Zhanga, N.; Hodgeb, B.M.; Kanga, C.; Kroposkib, B.; Xiaa, Q. Economic justification of concentrating solar power in high renewable energy penetrated power systems. *Appl. Energy* **2018**, *222*, 649–661. [CrossRef]
21. Gallego, A.J.; Camacho, E.F. Adaptative state-space model predictive control of a parabolic-trough field. *Control Eng. Pract.* **2012**, *20*, 904–911. [CrossRef]
22. Sánchez, A.J.; Gallego, A.J.; Escaño, J.M.; Camacho, E.F. Temperature homogenization of a solar trough field for performance improvement. *Sol. Energy.* **2018**, *165C*, 1–9. [CrossRef]
23. Atlantica. Our Assets: Mojave. 2018. Available online: https://www.atlanticayield.com/web/en/company-overview/our-assets/asset/Mojave/ (accessed on 1 September 2019).
24. USEPA. AVoided Emissions and geneRation Tool (AVERT). 2018. Available online: https://www.epa.gov/statelocalenergy/avoided-emissions-and-generation-tool-avert (accessed on 1 September 2019).

25. Technology, P. 2018. Available online: https://www.power-technology.com/projects/mojave-solar-thermal-power-california-us/ (accessed on 1 September 2019).

26. Carmona, R. Análisis, Modelado y Control de un Campo de Colectores Solares Distribuidos con Sistema de Seguimiento en un eje. Ph.D. Thesis, Universidad de Sevilla, Seville, Spain, 1985.

27. Berenguel, M. To the Control of Distributed Solar Collectors. Ph.D. Thesis, Universidad de Sevilla, Seville, Spain, 1996.

28. Reviriego, A.N.; del Olmo, F.H.; Álvarez-Barcia, L. Nonlinear Adaptive Control of Heat Transfer Fluid Temperature in a Parabolic Trough Solar Power Plant. *Energies* **2017**, *10*, 1155. [CrossRef]

29. Helios I. 2018. Available online: https://solarpaces.nrel.gov/helios-i (accessed on 6 September 2019).

30. Duffie, J.; Beckman, J. *Solar Engineering of Thermal Processes*, 2nd ed.; Wiley-Interscience: Hoboken, NJ, USA, 1991.

31. Stine, W.B.; Geyer, M. The Power from The Sun. 2001. Available online: http://www.powerfromthesun.net (accessed on 27 July 2019).

32. Gallego, A.J.; Yebra, L.J.; Camacho, E.F.; Sánchez, A.J. Mathematical Modeling of the Parabolic Trough Collector Field of the TCP-100 Research Plant. In Proceedings of the 9th EUROSIM Congress on Modelling and Simulation, Oulu, Finland, 12–16 September 2016.

33. Therminol VP1 HTF. 2018. Available online: https://www.therminol.com/products/Therminol-VP1 (accessed on 1 July 2019).

34. Sánchez, A.J.; Gallego, A.J.; Escaño, J.M.; Camacho, E.F. Event-based MPC for defocusing and power production of a parabolic trough plant under power limitation. *Sol. Energy* **2018**, *174*, 570–581. [CrossRef]

35. Akbarzadeh, S.; Valipour, M.S. Heat transfer enhancement in parabolic trough collectors: A comprehensive review. *Renew. Sustain. Energy Rev.* **2018**, *92*, 198–218. [CrossRef]

36. SCHOTT Solar CSP GmbH. SCHOTT PTR®70 Receivers. 2018. Available online: https://www.us.schott.com/csp/english/schott-solar-ptr-70-receivers.html (accessed on 1 July 2019).

37. Burkholder, F.; Brandemuehl, M.; Price, H.; Netter, J.; Kutscher, C.; Wolfrum, E. Parabolic Trough Receiver Thermal Testing. In Proceedings of the Energy Sustainability, ASME 2007 Energy Sustainability Conference, Long Beach, CA, USA, 27–30 July 2007; pp. 961–970. [CrossRef]

38. Camacho, E.F.; Rubio, F.R.; Berenguel, M.; Valenzuela, L. A survey on control schemes for distributed solar collector fields. Part I: Modeling and basic control approaches. *Sol. Energy* **2007**, *81*, 1240–1251. [CrossRef]

39. Robledo, M.; Escano, J.M.; Núñez, A.; Bordons, C.; Camacho, E.F. Development and Experimental Validation of a Dynamic Model for a Fresnel Solar Collector. *IFAC Proc. Vol.* **2010**, *44*, 483–488. [CrossRef]

40. Chaibakhsh, A.; Ghaffari, A. Steam Turbine Model. *Simul. Model. Pract. Theory* **2008**, *16*, 1145–1162. [CrossRef]

41. nes, R.M.M.; Windahlb, J.; Palssonb, J.; Thern, M. Dynamic Modeling of a Parabolic Trough Solar Thermal Power Plant with Thermal Storage Using Modelica. *Heat Transf. Eng.* **2018**, *39*, 277–292.

42. Ferruzza, D.; Topel, M.; Basaran, I.; Laumert, B.; Haglind, F. Start-Up Performance of Parabolic Trough Concentrating Solar Power Plants. *AIP Conf. Proc.* **2017**. [CrossRef]

43. Guidotti, R.; Monreale, A.; Ruggieri, S.; Turini, F.; Giannotti, F.; Predeschi, D. A Survey of Methods for Explaining Black Box Models. *ACM Comput. Surv.* **2018**, *51*, 1–42. [CrossRef]

44. Arendt, K.; Jradi, M.; Shaker, H.R.; Veje, C.T. Comparative analysis of white-, gray- and black-box models for thermal simulation of indoor environment: Teaching building case study. In Proceedings of the 2018 Building Performance Modeling Conference and SimBuild Co-Organized by ASHRAE and IBPSA-USA, Chicago, IL, USA, 26–28 September 2018.